SEMAC and MAVRIC for Artifact-Corrected MR Imaging around Metal in the Knee

C. A. Chen[1], W. Chen[2], S. B. Goodman[1], B. A. Hargreaves[1], K. M. Koch[3], W. Lu[1], A. C. Brau[2], C. E. Draper[1], S. L. Delp[1], and G. E. Gold[1]
[1]Stanford University, Stanford, CA, United States, [2]GE Healthcare Applied Science Lab, Menlo Park, CA, United States, [3]GE Healthcare Applied Science Lab, Milwaukee, WI, United States

INTRODUCTION

MRI is ideal for musculoskeletal imaging, due to its superb soft tissue contrast and three-dimensional reformatting ability. Unfortunately, post-surgical imaging around metal is often limited to plain radiography due to artifacts such as signal loss and distortion [1] which limit the diagnostic value of MRI for post-operative complications [2]. We have developed two 3D MR imaging prototypes that correct for these artifacts, Slice Encoding for Metal Artifact Correction (SEMAC) [3] and Multi-Acquisition Variable-Resonance Image Combination (MAVRIC) [4]. SEMAC corrects for distortion and artifact by building on the view-angle tilting technique [5] to align resolved excitation profiles to their actual voxel locations using additional phase encoding in the slice direction. MAVRIC minimizes distortion and artifact by limiting the excited bandwidth, then uses multiple resonant frequency offset acquisitions to cover the full spectral range. We compared artifact size measured on SEMAC and MAVRIC images to two-dimensional fast spin echo (FSE) [6] images of the knee in volunteers and patients with total knee replacements (TKR). Additionally, we compared the capabilities of SEMAC, MAVRIC, and FSE in accurately measuring geometry in the presence of metal in a TKR knee model.

METHODS

After obtaining informed consent and IRB approval, ten knees of nine volunteers with TKRs were imaged in the sagittal plane using a GE Signa HDx 1.5T MRI scanner and an 8-channel knee coil. All images were acquired with bandwidth +/-125Hz, slice thickness 3mm, and resolution 320x256. Field-of-view was adjusted for knee size. FSE was acquired with repetition time/echo time (TR/TE) =3000/6.4ms, 2 NEX, 36 slices, and an average scan time of 5 minutes. SEMAC was obtained with TR/TE=3446/11.3ms, 0.5 NEX, 2x auto calibrated parallel imaging (ARC) [7], 36 slices, and an average scan time of 8:23. MAVRIC was acquired with TR/TE=3650/39.6ms, 0.5 NEX, 2x ARC, 40 slices, and an average scan time of 11:23. SEMAC and MAVRIC images were both reconstructed using a sum-of-squares combination [4] (Fig. 1).

For each knee, the medial tibial plate, anterior medial femoral component, and posterior medial femoral component were evaluated for artifact. For each sequence, 3 slices equally spanning the medial-lateral dimension were chosen from which to measure the extent of the artifacts. After the same artifact was identified on all 3 sequences, the artifact extent was measured by a line perpendicular to the curvature of the metal component associated with the artifact. The extent of the artifact was measured using Osirix [8] (version 3.0.1) and compared among sequences with paired t-tests.

To evaluate the accuracy of the sequences in measuring geometry in the presence of metal, a model of the post-operative knee was made and scanned (Fig. 2). The model consisted of plastic femoral and tibial bones manufactured to fit a TKR with cobalt-chromium femoral component, plastic spacer, and stainless steel tibial component. The bones were drilled to hold cylinders of oil to simulate subchondral fat, and placed within a cylinder of water to simulate synovial fluid. The manufacturer's known maximum anterior/posterior (A/P) and medial/lateral (M/L) dimensions of the metal femoral and tibial components and plastic spacer were compared to the dimensions measured by the 3 sequences through percent deviations.

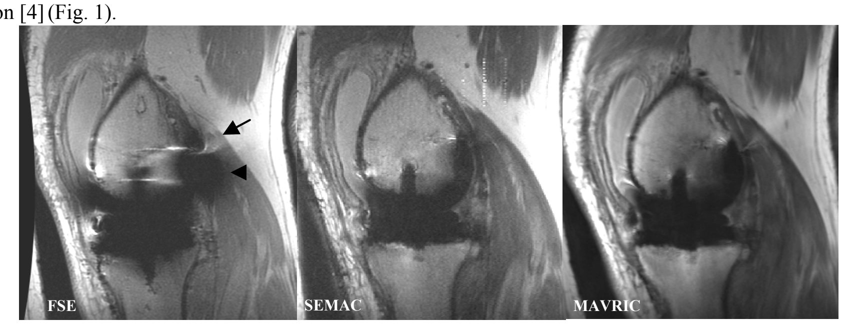

Figure 1: Sagittal MR images of a TKR. MAVRIC and SEMAC correct metal-induced distortion (as example, arrow) and artifact (arrowhead) that limit the diagnostic value of FSE images.

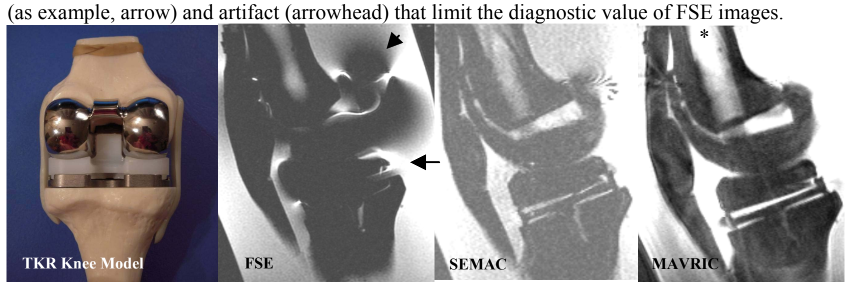

Figure 2: (*Left*) Posterior view of TKR model of the knee, consisting of plastic bones filled with oil (*) and fitted to metal components. (*Right*) Sagittal MR images of the TKR knee model. FSE images had severe metal-induced distortion (arrow) and artifact (arrowhead).

RESULTS

In all metal joint compartments, SEMAC and MAVRIC were both significantly better at artifact reduction than FSE (all $P<.01$), while being statistically equivalent to each other (all $P>.07$, Fig. 3). For the model of the knee, SEMAC and MAVRIC enabled more accurate measurements of metallic implant geometry than FSE (Table 1).

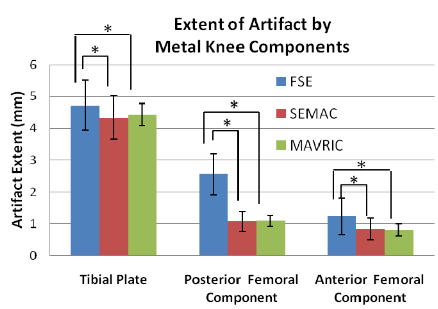

Figure 3: SEMAC and MAVRIC images had significantly less artifact than conventional FSE images, while being statistically similar to each other. * = $P<.05$.

TKR Component	Percent Deviation (%) between Measured and Known TKR Dimensions		
	FSE	*SEMAC*	*MAVRIC*
A/P Femur	+24.8	-3.4	-3.6
M/L Femur	+16.8	+2.0	+0.4
A/P Tibia	-1.6	-4.6	-1.8
M/L Tibia	+7.5	-2.2	+3.4
A/P Spacer	+10.8	-4.5	-5.1
M/L Spacer	+17.0	+1.0	+1.3

Table 1: SEMAC and MAVRIC had much smaller deviations from actual component dimensions than FSE, indicating their accuracy in measuring metallic implant geometry.

DISCUSSION

Results from the human volunteers and TKR knee model demonstrate that both SEMAC and MAVRIC correct for metal-induced distortion and artifact, allowing them to accurately measure metal implant geometry. FSE images suffered from statistically larger artifacts, particularly around the femoral component.

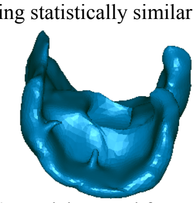

Figure 4: Model created from segmentation of femoral TKR component from SEMAC images.

CONCLUSION

SEMAC and MAVRIC are promising MR imaging techniques that allow for improved assessment of bone and soft tissue structures surrounding metal in the knee.

ACKNOWLEDGEMENTS NIH grants R21-EB008190, 1R01-EB002524, 1R01-EB005790; The Wallace H. Coulter Foundation; GE Healthcare.

REFERENCES

1. Wendt RE et al., Radiology 1988;168:837-41.
2. Sofka et al., Semin Musculoskel Radiol 2002;6:79-85.
3. Lu W et al., Magn Res Med 2009;62(1):66-76.
4. Koch KM et al., Magn Reson Med 2009;61(2):381-90.
5. Jee et al., Am J Roentgenol 2003;180:93-7.
6. Hennig J., Magn Reson Med 1986;3(6):823-33.
7. Beatty et al., Proc. ISMRM-ESMRMB p. 1749, 2007.
8. Rosset et al., J Digit Imaging 2004;17(3):205-16.